Rapid Turnover of Effector–Memory CD4^{+} T Cells in Healthy Humans

Derek C. Macallan,[1] Diana Wallace,[2] Yan Zhang,[1] Catherine de Lara,[2]
Andrew T. Worth,[2] Hala Ghattas,[1] George E. Griffin,[1]
Peter C.L. Beverley,[2] and David F. Tough[2]

[1]*Department of Infectious Diseases, St. George's Hospital Medical School, London SW17 0RE, UK*
[2]*Edward Jenner Institute for Vaccine Research, Compton, Newbury, Berkshire RG20 7NN, UK*

Abstract

Memory T cells can be divided into central–memory (T_{CM}) and effector–memory (T_{EM}) cells, which differ in their functional properties. Although both subpopulations can persist long term, it is not known whether they are maintained by similar mechanisms. We used in vivo labeling with deuterated glucose to measure the turnover of CD4^{+} T cells in healthy humans. The CD45R0^{+}CCR7^{−} T_{EM} subpopulation was shown to have a rapid proliferation rate of 4.7% per day compared with 1.5% per day for CD45R0^{+}CCR7^{+} T_{CM} cells; these values are equivalent to average intermitotic (doubling) times of 15 and 48 d, respectively. In contrast, the CD45RA^{+}CCR7^{+} naive CD4^{+} T cell population was found to be much longer lived, being labeled at a rate of only 0.2% per day (corresponding to an intermitotic time of approximately 1 yr). These data indicate that human CD4^{+} T_{EM} cells constitute a short-lived cell population that requires continuous replenishment in vivo.

Key words: T lymphocyte • immune memory • homeostasis • cell proliferation • cell lifespan

Introduction

One factor contributing to immunological memory is the much higher frequency of lymphocytes specific for the priming antigen in the memory pool than among naive cells. Long-term persistence of memory cells is achieved by a combination of two processes: first, the long-term survival of individual cells, and second, periodic cell division to balance attrition through cell death. Both processes are dependent on contact with MHC–peptide complexes and with cytokines such as IL-15 and IL-7 (1). Current understanding of how memory cell populations persist has been aided by studies investigating the kinetic behavior of T cells in various animal species, including humans, which have shown that those cells with a memory phenotype (CD45R0[+] in humans) exhibit a considerably higher rate of turnover than naive phenotype T cells and have a relatively short lifespan, on the order of weeks or months (2–7). However, memory T cells are phenotypically and functionally heterogeneous, and it is not known if rapid turnover applies to all memory cells.

A major subdivision among memory T cells is that between central–memory (T_{CM}) and effector–memory (T_{EM}) cells

(8). These subpopulations, which are identified among human CD45R0^{+} T cells as being CCR7^{+}CD62L^{+} or CCR7^{−}CD62L^{−} respectively, exhibit distinct functional properties. T_{CM} cells enter LNs through high endothelial venules and recirculate primarily between blood and lymph, whereas T_{EM} cells migrate preferentially from the blood into peripheral tissues such as the lung or intestinal mucosa (9–11). In addition, T_{EM} cells express effector activity (e.g., cytolytic activity or secretion of cytokines such as IFN-γ, IL-4, or IL-5) more rapidly than T_{CM} cells upon restimulation with antigen (8, 9, 12), although some studies suggest that this distinction may be less clear for memory CD8^{+} T cells (13). On this basis, T_{CM} and T_{EM} cells have been proposed to play complementary roles in the secondary response to infection, with T_{EM} cells providing a rapid effector response at sites of pathogen entry and T_{CM} cells serving as an expanded pool of precursors that can proliferate in the secondary lymphoid organs to rapidly generate large numbers of effector cells (8).

Although both T_{CM} and T_{EM} CD4^{+} populations appear to persist long term in humans (8), the kinetic behavior of the cells which comprise these subpopulations is unknown. To measure turnover of human T_{CM} and T_{EM} CD4^{+} cells, we used [2]H-glucose, which is incorporated into DNA via the de novo nucleotide synthesis pathway, to label dividing

Address correspondence to David F. Tough, Edward Jenner Institute for Vaccine Research, High St., Compton, Newbury, Berkshire RG20 7NN, UK. Phone: 44-1635-577915; Fax: 44-1635-577901; email: david.tough@jenner.ac.uk

cells in vivo (14). The results show a clear difference in turnover rates between these subpopulations, with T_{EM} CD4$^+$ cells being much shorter lived. The implications for maintenance of T cell memory are discussed.

Materials and Methods

In Vivo Labeling with $^2H_2$-Glucose. Six young healthy volunteers (ranging from 19 to 30 yr of age) were given a primed 24-h i.v. infusion of $\sim$1 g/kg 6,6-$^2H_2$-glucose (Cambridge Isotopes). During this time, their diet was restricted to small, low energy meals. For measurement of plasma glucose ^2H enrichment, blood was taken at $\sim$4-hr intervals during infusion. For estimation of ^2H enrichment in cell DNA, 50 ml heparinized blood samples were taken at 3, 4, 10, and 21 d after commencement of the infusion. All subjects gave written informed consent under protocols approved by the Local Research Ethics Committee.

Cell Sorting. PBMCs were isolated from blood by Ficoll-Paque (Amersham Biosciences) density gradient centrifugation and stained (10^7/ml in PBS + 0.2% BSA) in one of three ways. (i) Mouse anti–human CCR7 (IgM) (BD Biosciences), goat anti–mouse IgM F(ab$'$)$_2$-RPE (Southern Biotechnology Associates Inc.), anti–CD45RA-RPE-CY5 (Serotec Ltd.) and anti–CD4–APC (BD Biosciences). (ii) Anti–human CCR7, anti-IgM (Fab)$_2$-PE, anti-CD45RA-biotin (BD Biosciences), streptavidin-PerCP (BD Biosciences), and anti–CD4–APC. (iii) Anti–human CCR7, anti-IgM (Fab)$_2$-PE, anti–CD4-biotin (BD Biosciences), streptavidin-PerCP, anti-CD45R0-allophycocyanin (CALTAG). Similar results were obtained using any of these staining strategies. Stained cells were sorted using a Moflow flow cytometer (Cytomation). Typical purities and cell yields for the three major subpopulations (naive, T_{CM}, T_{EM}) were 85–98% and 1–6 × 10^6, respectively; much smaller numbers of RA$^+$7$^-$ cells were obtained ($\sim$4 × 10^5), and purity was usually lower than for the other three populations.

Analysis of Deuterium Enrichment and Modeling of Proliferation. Enrichment of deuterium in DNA was assayed essentially as described previously (7, 15). Briefly, cellular DNA was extracted and digested enzymatically to deoxynucleosides. Purified deoxyadenosine was converted to its aldonitrile triacetate derivative by reaction with hydroxylamine/pyridine and acetic anhydride. The resulting derivative was analyzed in triplicate by gas chromatography mass spectrometry, monitoring ions m/z 198 and 200 (SIM mode in PCI, HP-225 column, HP 6890/5973 GCMS; Hewlett Packard). Typical precision of reproducibility of the M+2 to M+0 ratio was ±0.02%. Plasma glucose enrichment was measured using the same derivatization (m/z 328 and 330). For each subject, mean glucose enrichment for the 24-h labeling period was derived from the area under the curve for the enrichment time profile. Mean glucose enrichment ranged from 18 to 29% (mean 24%).

Results were expressed as the fraction of labeled cells (F) present on each day, given by the ratio of the enrichment of label in DNA (E) and the precursor enrichment (b, the mean glucose enrichment over 24 h × 0.65) (14). The magnitude of the peak value for F represents a crude measure of the cellular proliferation rate. Data was modeled as previously described (7) (Sigmaplot v8.02; SPSS), to estimate the rate of proliferation during labeling, p, and subsequent rate of loss of labeled cells, d*, taking into account cell death between the end of labeling and first sampling on day 3 and assuming no changes in pool sizes, according to the following equations:

$$F(t) = \frac{p}{d^*}(1 - e^{-d^*t}) \qquad t \leq \tau \quad \text{during the labeling period}$$

$$F(t) = \frac{p}{d^*}(1 - e^{-d^*\tau})e^{-d^*(t-\tau)} \quad t > \tau \quad \text{after the labeling period}$$

where t is time and τ is the length of the labeling period.

In this model, no assumption of equality between p and d* has been made; p represents the average proliferation rate of the whole population, whereas d* refers only to labeled cells (i.e., cells which divided during the labeling period). For a kinetically heterogeneous population, even one at steady-state, these two rates will not be the same, as discussed elsewhere (7). Where the day 3 value fell below the day 4 value for the same lymphocyte pool, it was assumed that the day 3 value lay within the lag phase between division and appearance in the circulation, and it was excluded from modeling. Where proliferation is expressed as doubling time (t_2) or disappearance as half-life ($t_{1/2}$), these were calculated as ln2/p and ln2/d, respectively. Data are expressed as means. Comparisons between groups were made by Student's t test.

Results and Discussion

To measure T cell turnover in vivo, healthy volunteers were infused with ^2H-labeled glucose for 24 h, and enrichment of ^2H in the DNA of isolated subpopulations of peripheral blood lymphocytes was determined at several time points. Day 3 was chosen as the earliest time point since previous work has shown that the appearance of labeled T cells in the blood peaks at $\sim$3–4 d after starting the infusion (7). CD4$^+$CD3$^+$ cells were subdivided by cell sorting into four populations: CD45R0$^+$ (or CD45RA$^-$) CCR7$^+$ T_{CM} cells, CD45R0$^+$ (or CD45RA$^-$) CCR7$^-$ T_{EM} cells, CD45R0$^-$ (or CD45RA$^+$) CCR7$^+$ naive cells and CD45R0$^-$ (or CD45RA$^+$) CCR7$^-$ cells (referred to as RA$^+$7$^-$ cells). Lack of CCR7 expression on the latter subset, which represents a small fraction of total CD45RA$^+$ CD4$^+$ T cells, suggests that RA$^+$7$^-$ cells are not naive; antigen-primed cells have been identified previously among CD45RA$^+$ CD4$^+$ cells based on an absence of CD31 expression (16). On average, these subpopulations represented $\sim$21% (T_{CM}), 12% (T_{EM}), 64% (naive), and 3% (RA$^+$7$^-$) of total peripheral blood CD4$^+$ T cells in the subjects studied.

From the measurement of ^2H enrichment in DNA, the proportion of cells in each subpopulation that was labeled at the different time points was calculated, and these values are shown in Fig. 1. Based on the results, several points can be made. First, labeling of naive cells was extremely low, confirming previous work showing that there is little proliferation within this subpopulation (2–7). Second, labeling of T_{EM} cells occurred at a substantially higher rate than for T_{CM} cells. This was observed clearly in five of the six subjects studied. In the sixth subject (C15), similar rates of labeling were observed for T_{EM} and T_{CM} cells, which appeared to be due to a higher than average labeling of T_{CM} cells in this individual. Third, RA$^+$7$^-$ cells showed a relatively rapid rate of labeling, consistent with the view that these cells are not naive but rather are antigen-primed; the exact relationship

CD45RA+ CD45R0+
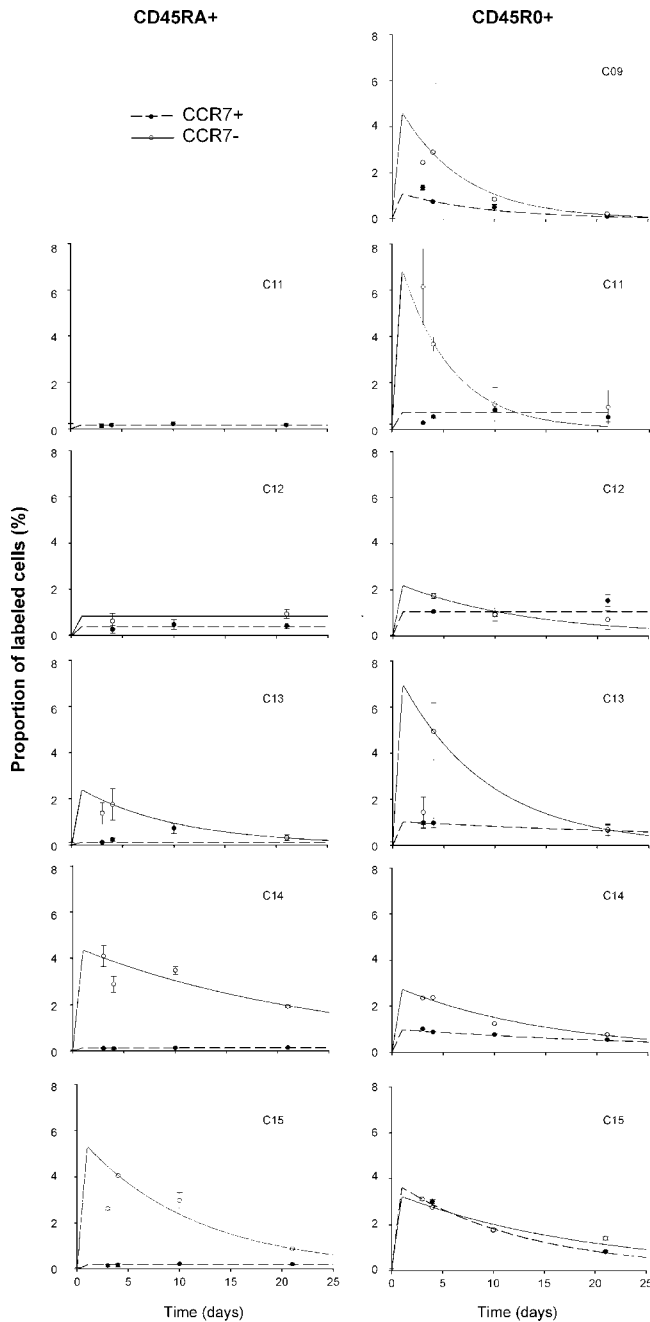
Figure 1. Kinetics of labeling of naive, T_{CM}, T_{EM}, and RA+7− CD4+ T cells after infusion of ^{2}H-glucose. Subjects were infused with ^{2}H-glucose for 24 h starting from time 0, and the proportion of labeled cells (relative to total cells in each subpopulation) at different time points is shown for CD45RA+ (left) and CD45R0+ CD4+ T cells (right). Data for CCR7+ and CCR7− cells are indicated by filled or open symbols, respectively; error bars represent the SD of triplicate GCMS measurements. Lines represent best-fit curves calculated based on the data points and assuming maximal labeling at 24 h.

between these cells and T_{CM} or T_{EM} cells remains to be defined. Peak height values (the maximum measured fraction of labeled cells) for each subpopulation are summarized in Table I. Mean values were higher in CCR7− than CCR7+ populations for both CD45R0+ and CD45RA+ cells.

Table I. *Glucose Enrichment and Peak Fraction of Labeled Cells after 24 h 6,6-D$_2$-Glucose*

| | Glucose enrichment[a] | Peak fraction of labeled cells[b] | | | |
| | | CD45R0+ | | CD45RA+ | |
		CCR7+	CCR7−	CCR7+	CCR7−
	$\% \cdot d$	$\%$	$\%$	$\%$	$\%$
C09[c]	29	1.4	2.9	ND	ND
C11[d]	25	0.8	6.1	0.2	ND
C12[e]	22	1.5	1.7	0.5	0.9
C13[e]	18	1.0	4.9	0.7	1.7
C14[e]	28	1.0	2.4	0.1	4.1
C15[e]	20	3.0	3.1	0.2	4.1
Mean	24	1.5	3.5[f]	0.3	2.7[f]
SD	5	0.8	1.7	0.2	1.6

[a]From area under curve of enrichment time profile.
[b]Maximal value for labeling expressed as F (fraction of labeled cells) measured in lymphocyte subpopulations at time points sampled. Cells were sorted according to method i[c], ii[d], or iii[e] (see Materials and Methods).
[f]P < 0.05 for CCR7+ versus CCR7− by paired Student's *t* test.

To determine the rates of proliferation (p) and disappearance (d*) for the various cell subpopulations, curves were fitted to the data based on the fraction of labeled cells detected at each time point (Fig. 1). Note that in modeling the data it was assumed that maximal labeling was present at 24 h (i.e., at the cessation of ^{2}H infusion) and that label disappeared exponentially thereafter with a disappearance rate constant, d*; this model takes into account cell death between the end of labeling and first sampling on day three. As shown in Table II, p was significantly higher for T_{EM} than T_{CM} cells. For the five subjects where this was the case, p for T_{EM} cells was on average five times of that of p for T_{CM} cells; T_{EM} and T_{CM} cells had roughly equivalent proliferation rates in the sixth subject. Overall, the average proliferation rates for T_{CM} and T_{EM} cells were ∼1.5 and 4.7% per day, respectively. From p, the average intermitotic time for cells within that population (t_2) can be calculated, yielding values of 48 d for T_{CM} cells and 15 d for T_{EM} cells.

Disappearance rates, though more variable, were also higher for T_{EM} than T_{CM} cells in five of the six subjects. On average, the disappearance rates were 4.1% per day for T_{CM} cells and 11.3% per day for T_{EM} cells (equivalent to half-lives [$t_{1/2}$] for disappearance of the cells of 17 and 6 d, respectively). Note that d* is a measure of the disappearance rate of labeled cells only, whereas p applies to all cells, explaining why d* can exceed p at steady-state (even though d, the disappearance rate of the entire population, must equal p). As discussed previously, several explanations can be proposed for the relatively rapid disappearance of recently divided cells (7). Although this was true for both

257 Macallan et al. Brief Definitive Report

Table II. *Proliferation and Disappearance Rates for T_{CM}, T_{EM}, Naive, and RA^+7^- $CD4^+$ T Cells*

	Proliferation				Disappearance			
	CCR7$^+$		CCR7$^-$		CCR7$^+$		CCR7$^-$	
				CD45R0$^+$				
Subject	p	t$_2$	p	t$_2$	d*	t$_{1/2}$	d*	t$_{1/2}$
%/day	*%/day*	*days*	*%/day*	*days*	*%/day*	*days*	*%/day*	*days*
C09	1.15	60	5.01	14	11.53	6.0	16.16	4.3
C11	0.74	94	7.59	9	0.00	>^{c}	20.28	3.4
C12	1.05	66	2.27	31	0.00	>	8.00	8.7
C13	1.03	67	7.41	9	2.32	29.9	11.61	6.0
C14	1.00	69	2.83	24	3.20	21.7	6.56	10.6
C15	3.77	18	3.31	21	7.74	9.0	5.26	13.2
Mean	1.46	48	4.74^a	15	4.13	17	11.31^a	6
± SD	±1.14		±2.33		±4.61		±5.90	
				CD45RA$^+$				
C11	0.16	433	ND^b	ND	0.00	>	ND	ND
C12	0.37	187	0.84	83	0.00	>	0.00	>
C13	0.11	630	2.51	28	0.00	>	10.35	6.7
C14	0.12	578	4.44	16	0.00	>	4.02	17.2
C15	0.20	347	5.56	12	0.00	>	8.95	7.7
Mean	0.19	361	3.34^a	21	0.00	>	5.83^a	12
±SD	±0.11		±2.09		±0.00		±4.74	

Values for proliferation (p) and disappearance (d*) rates were derived from the best fit curves applied to the data (see Materials and Methods). t$_2$ and t$_{1/2}$ represent doubling time or half-life equivalents of p or d*, respectively; mean values for t$_2$ and t$_{1/2}$ are calculated from the mean values for p and d*, respectively.
[a]$P < 0.05$ for CCR7$^+$ versus CCR7$^-$ by paired Student's *t* test.
[b]ND indicates not determined because of inadequate data for model estimate.
[c]> indicates t$_2$ or t$_{1/2}$ exceeds maximal value detectable (p or d* close to zero).

T_{EM} and T_{CM} cells in many subjects, it is notable that labeled T_{CM} cells in two individuals exhibited negligible disappearance rates, implying that some T_{CM} cells can differentiate into long-lived cells after division. In contrast, d* was higher than p for T_{EM} cells in all subjects.

For naive CD4$^+$ T cells, p was very low, ~0.2% per day, which converts to a t$_2$ for the naive population of about a year (Table II). This contrasts with the rapid proliferation observed among RA$^+7^-$ cells, which had an average p of 3.3% per day (t$_2$ = 21 d). The labeling that does occur amongst truly naive CD4$^+$ T cells could reflect division of precursors in the thymus and their release into the blood over the time course of the analysis. Alternatively, some proliferation of mature naive cells could occur in the secondary lymphoid organs, perhaps in response to contact with homeostatic cytokines (17–21). Whichever the case, however, it is evident that the contribution of cell division

to maintaining the naive CD4$^+$ T cell pool in young adults is minimal.

In addition, the disappearance rate for the majority of naive (CD45RA$^+$CCR7$^+$) CD4$^+$ T cells was shown to be extremely slow. In fact, we found that d* for CD45RA$^+$CCR7$^+$ cells in all subjects was too small to estimate using this method. This contrasts with earlier results showing a relatively rapid disappearance rate for labeled total CD4$^+$CD45RA$^+$ cells of >7% per day (7). This disparity may be partly explained by the disproportionate contribution of RA$^+7^-$ cells to labeling in the previous study, since labeled cells in this population disappear rapidly. The present data are striking in their implication that human naive CD4$^+$ T cells can remain in interphase for extremely long periods of time after their derivation from dividing precursors.

Overall, the relative quiescence of naive CD4$^+$ T cells and rapid turnover of memory–phenotype cells reported

here are in agreement with the general pattern of kinetic behavior that has been observed for these cells in many different species. Our data show that T_{CM} and T_{EM} CD4^{+} T cells in humans have distinct rates of turnover, with T_{EM} cells typically being replaced at a much faster rate than T_{CM} cells. These results imply that an almost continuous input of new cells is required to maintain the T_{EM} CD4^{+} T cell population, which could have important implications for vaccination given that T_{EM} may serve to provide a rapid effector response to reinfection. At face value, it could be argued that the shorter lifespan observed for T_{EM} cells in the blood is simply a consequence of these cells having an ability to migrate rapidly and irreversibly into tissues. However, if one assumes that the number of T_{EM} cells in tissues is constant (rather than increasing) under steady-state conditions, turnover of cells in the blood ultimately reflects what is occurring in the total T_{EM} population. Therefore, it is evident from the rapid rate of production that there is also a rapid rate of disappearance among T_{EM} cells.

Several factors could contribute to differences in the kinetic behavior between T_{CM} and T_{EM} cells. First, their distinct patterns of migration make it likely that the extent to which they contact cell division- and survival-inducing factors will differ (22). Second, it has been shown that T_{CM} and T_{EM} cells exhibit intrinsic differences in their responsiveness to homeostatic cytokines (23). In particular, T_{EM} cells have higher cell surface expression of the IL-2/IL-15R β-chain, allowing them to proliferate in response to lower concentrations of IL-15 than T_{CM} cells. This difference could potentially account for the higher proliferation rate among T_{EM} cells. Third, T_{EM} and T_{CM} cells may also differ in their intrinsic death rates or their ability to respond to survival factors.

The present data should be considered with respect to the uncertainty that exists in understanding the lineage relationship between T_{CM} and T_{EM} cells, specifically whether these cells represent independent subpopulations or merely different activation states along a common differentiation pathway. Previous work has shown that phenotypic conversion can take place between T_{CM} and T_{EM} cells, suggesting that one subpopulation could serve as a source for the other; this has been observed for human CD4^{+} cells, where T_{CM} cells can acquire characteristics of T_{EM} cells in response to stimulation through the TCR or by cytokines (23), and in the reverse direction for mouse CD8^{+} T cells, where virus-specific T_{EM} cells were shown to convert to T_{CM} cells with time after infection (24). In contrast, based on analysis of T cell clonotypes present among T_{CM} and T_{EM} CD8^{+} T cells it was concluded that these cells represent independently regulated cell subpopulations in humans (25). Although the present kinetic data could indicate that T_{CM} and T_{EM} cells are maintained as separate pools with distinct turnover rates, they are also compatible with a model in which interconnection of T_{CM} and T_{EM} cells occurs in both directions. According to this latter model, T_{EM} cells are maintained primarily through cell division, either by existing T_{EM} cells or by T_{CM} cells that acquire a T_{EM} phenotype concomitant with division. Replacement of T_{CM} cells would occur through more limited cell division among T_{CM} cells that do not change phenotype and by phenotypic reversion of T_{EM} cells after these cells have returned to a quiescent state. Future studies will be required to distinguish between the two models.

Finally, these results raise the question of whether further heterogeneity exists in the kinetic behavior of human CD4^{+} T cells. Previously, evidence for kinetic heterogeneity amongst antigen-primed human CD4^{+} T cells had been suggested by analysis of total memory–effector-phenotype CD4^{+} T cells (26). By using CCR7 as a marker, we were able to demonstrate that there are distinct subpopulations with differing turnover rates present in both CD45RA^{+} and CD45R0^{+} CD4^{+} T cell populations. In the future, it will be of interest to use other cell surface markers, for example, those associated with recent activation, to characterize the in vivo behavior of additional cell populations.

References

1. Schluns, K.S., and L. Lefrancois. 2003. Cytokine control of memory T-cell development and survival. *Nat. Rev. Immunol.* 3:269–279.
2. Mackay, C.R., W.L. Marston, and L. Dudler. 1990. Naive and memory T cells show distinct pathways of lymphocyte recirculation. *J. Exp. Med.* 171:801–817.
3. Michie, C.A., A. McLean, A. Alcock, and P.C.L. Beverley. 1992. Lifespan of human lymphocyte subsets defined by CD45 isoforms. *Nature.* 360:264–265.
4. Tough, D.F., and J. Sprent. 1994. Turnover of naive- and memory-phenotype T cells. *J. Exp. Med.* 179:1127–1135.
5. Mohri, H., S. Bonhoeffer, S. Monard, A.S. Perelson, and D.D. Ho. 1998. Rapid turnover of T lymphocytes in SIV-infected Rhesus Macaques. *Science.* 279:1223–1227.
6. McCune, J.M., M.B. Hanley, D. Cesar, R. Halvorsen, R. Hoh, D. Schmidt, E. Eieder, S. Deeks, S. Siler, and R. Neese. 2000. Factors influencing T-cell turnover in HIV-1-seropositive patients. *J. Clin. Invest.* 105:R1–R8.
7. Macallan, D.C., B. Asquith, A.J. Irvine, D.L. Wallace, A. Worth, H. Ghattas, Y. Zhang, G.E. Griffin, D.F. Tough, and P.C. Beverley. 2003. Measurement and modelling of human T cell kinetics. *Eur. J. Immunol.* 33:2316–2326.
8. Sallusto, F., D. Lenig, R. Forster, M. Lipp, and A. Lanzavecchia. 1999. Two subsets of memory T lymphocytes with distinct homing potentials and effector functions. *Nature.* 401:708–712.
9. Masopust, D., V. Vezys, A.L. Marzo, and L. Lefrancois. 2001. Preferential localization of effector memory cells in nonlymphoid tissue. *Science.* 291:2413–2416.
10. Reinhardt, R.L., A. Khoruts, R. Merica, T. Zell, and M.K.

Jenkins. 2001. Visualizing the generation of memory CD4 T cells in the whole body. *Nature*. 410:101–105.

11. Weninger, W., M.A. Crowley, N. Manjunath, and U.H. von Andrian. 2001. Migratory properties of naive, effector, and memory CD8^{+} T cells. *J. Exp. Med*. 194:953–966.

12. Hislop, A.D., N.H. Gudgeon, M.F.C. Callan, C. Fazou, H. Hasegawa, M. Salmon, and A.B. Rickinson. 2001. EBV-specific CD8^{+} T cell memory: relationships between epitope specificity, cell phenotype, and immediate effector function. *J. Immunol*. 167:2019–2029.

13. Champagne, P., G.S. Ogg, A.S. King, C. Knabenhans, K. Ellefsen, M. Nobile, V. Appay, G.P. Rizzardi, S. Fleury, M. Lipp, et al. 2001. Skewed maturation of memory HIV-specific CD8 T lymphocytes. *Nature*. 410:106–111.

14. Macallan, D.C., C.A. Fullerton, R.A. Neese, K. Haddock, S.S. Park, and M.K. Hellerstein. 1998. Measurement of cell proliferation by labeling of DNA with stable isotope-labeled glucose: studies in vitro, in animals and in humans. *Proc. Natl. Acad. Sci. USA*. 95:708–713.

15. Neese, R.A., S.Q. Siler, D. Cesar, F. Antelo, D. Lee, L. Misell, K. Patel, S. Tehrani, P. Shah, and M.K. Hellerstein. 2001. Advances in the stable isotope-mass spectrometric measurement of DNA synthesis and cell proliferation. *Anal. Biochem*. 298:189–195.

16. Thiel, A., J. Schmitz, S. Miltenyi, and A. Radbruch. 1997. CD45RA-expressing memory/effector Th cells committed to production of interferon-γ lack expression of CD31. *Immunol. Lett*. 57:189–192.

17. Soares, M.V.D., N.J. Borthwick, M.K. Maini, G. Janossy, M. Salmon, and A.N. Akbar. 1998. IL-7-dependent extrathymic expansion of CD45RA^{+} T cells enables preservation of a naive repertoire. *J. Immunol*. 161:5909–5917.

18. Schluns, K.S., W.C. Kieper, S.C. Jameson, and L. Lefrancois. 2000. Interleukin-7 mediates the homeostasis of naive and memory CD8 T cells in vivo. *Nat. Immunol*. 1:426–432.

19. Fry, T.J., M. Moniuszko, S. Creekmore, S.J. Donohue, D.C. Douek, S. Giardina, T.T. Hecht, B.J. Hill, K. Komschlies, J. Tomaszewski, et al. 2003. IL-7 therapy dramatically alters peripheral T-cell homeostasis in normal and SIV-infected non-human primates. *Blood*. 101:2294–2299.

20. Schonland, S.O., J.K. Zimmer, C.M. Lopez-Benitez, T. Widmann, K.D. Ramin, J.J. Goronzy, and C.M. Weyand. 2003. Homeostatic control of T-cell generation in neonates. *Blood*. 102:1428–1434.

21. O'Neill, R.M., J. Hassan, and D.J. Reen. 2003. IL-7-regulated homeostatic maintenance of recent thymic emigrants in association with caspase-mediated cell proliferation and apoptotic cell death. *J. Immunol*. 170:4524–4531.

22. Harris, N.L., V. Watt, F. Ronchese, and G. Le Gros. 2002. Differential T cell function and fate in lymph node and non-lymphoid tissues. *J. Exp. Med*. 195:317–326.

23. Geginat, J., F. Sallusto, and A. Lanzavecchia. 2001. Cytokine-driven proliferation and differentiation of human naive, central memory, and effector memory CD4^{+} T cells. *J. Exp. Med*. 194:1711–1719.

24. Wherry, E.J., V. Teichgraber, T.C. Becker, D. Masopust, S.M. Kaech, R. Antia, H. von Adrian, and R. Ahmed. 2003. Lineage relationship and protective immunity of memory CD8 T cell subsets. *Nat. Immunol*. 4:225–234.

25. Baron, V., C. Bouneaud, A. Cumano, A. Lim, T.P. Arstila, L. Ferradini, and C. Pannetier. 2003. The repertoires of circulating human CD8^{+} central and effector memory T cell subsets are largely distinct. *Immunity*. 18:193–204.

26. Hellerstein, M.K., R.A. Hoh, M.B. Hanley, D. Cesar, D. Lee, R.A. Neese, and J.M. McCune. 2003. Subpopulations of long-lived and short-lived T cells in advanced HIV-1 infection. *J. Clin. Invest*. 112:956–966.